JOURNAL OF MATERIALS SCIENCE 25 (1990) 2655–2666

Review
Twinning in ferroelectric and ferroelastic ceramics: stress relief

G. ARLT
Institut für Werkstoffe der Elektrotechnik, Aachen University of Technology, Aachen, FRG

The regular twinning in ceramics and metals below the temperature of a ferroelastic or ferroelectric structural phase transition is a result of energy minimization. Here homogeneous elastic energy is reduced at the expense of twin wall energy. The twin density depends on the grain size g; under homogeneous stress the total elastic energy of a grain increases $\propto g^3$. Any kind of twin wall, however, increases $\propto g^2$. Below the intersection of these two curves, stress reduction by twinning cannot lower the total energy. Thus there is a critical grain size below which twinning should not occur. Above this limit the width of the twin lamellae increases $\propto g^{1/2}$. The shape of the grain then adjusts to the surroundings in two dimensions only. Above another larger critical grain size more complex interfaces with higher surface energy are created, which allow stress relief in the third dimension. A semi-quantitative model is developed with the example of $BaTiO_3$ ceramic, of which the domain patterns are well known. It is representative for many ceramics. The high T_c superconductor $YBa_2Cu_3O_{7-\delta}$ also twins according to the same law. For three-dimensional adjustment here a proper interface is missing.

1. Introduction

Many reviews have been published on various aspects of twinning and on the nature of twin boundaries of minerals and of metals (e.g. [1–3]). In particular, twinning as a consequence of a phase transformation which leads to a small structural change of the lattice cell has been described extensively as mechanical twinning [1, 4] or as martensitic transformation [3].

Aizu's [5, 6] definition of the ferroelastic phase transition overlaps to a great extent with the generalized martensitic transition as mainly used by scientists in metallurgy. Metals with martensitic transitions often show stress–strain hysteresis curves (e.g. [2, 7]) as required by Aizu for ferroelastic materials.

Transitions which are assisted by diffusion in some cases also cause twinning. An example is the tetragonal–orthorhombic (t–o) transition of the high-T_c superconductor $YBa_2Cu_3O_{7-\delta}$ which requires diffusion of oxygen into the lattice (e.g. [8, 9]).

Numerous polycrystalline metals and ceramics which undergo the transformations described above have a simple lamellar twinning or a banded twin structure as shown schematically in Fig. 1. In this paper these structures will be discussed as favourable states of low energy.

The physical origin of this mechanical twinning has been ascribed by most authors (e.g. [1]) to a reduction of the mechanical stress fields. Thus mechanical twinning in ferroelastic ceramics or related materials can be compared with ferromagnetic or ferroelectric domain formation. In the magnetic case, magnetic field energy is reduced by the existence of magnetic domains at the expense of domain wall energy such that the sum of the two becomes a minimum. In the ferroelectric case the electric field energy is often reduced at the expense of domain wall energy in order to minimize the sum of the two. In ferroelastic materials it is the sum of elastic energy and domain wall or interface energy which becomes a minimum. The equilibrium configuration of the twin pattern, however, is established only if the walls have sufficient mobility or if the displaced atoms have sufficient time to establish or at least to attempt to reach a thermodynamic equilibrium.

The above comparison of the three groups is simplified because in the ferromagnetic and ferroelectric cases, in addition to the magnetic and electric fields, the elastic fields can also be significant or even dominant in determining the minimum of energy. Similarly, in ferroelastics which are polar or even magnetic, electric and magnetic field energies can contribute to the energy minimization. When the formation of the domain pattern is governed by stress fields they will be called mechanical or elastic domains by analogy with the magnetic and electric domains in ferromagnetic and ferroelectric materials. In this paper the words twin or domain and twin boundary, domain wall or interface will be used in a generalized sense.

The general formalism is the energy minimization

$$w_{tot} = w_M + w_E + w_W + w_S = \text{minimum}$$

with w_M = elastic energy, w_E = electric energy, w_W = domain wall (or interface) energy and

0022–2461/90 $03.00 + .12

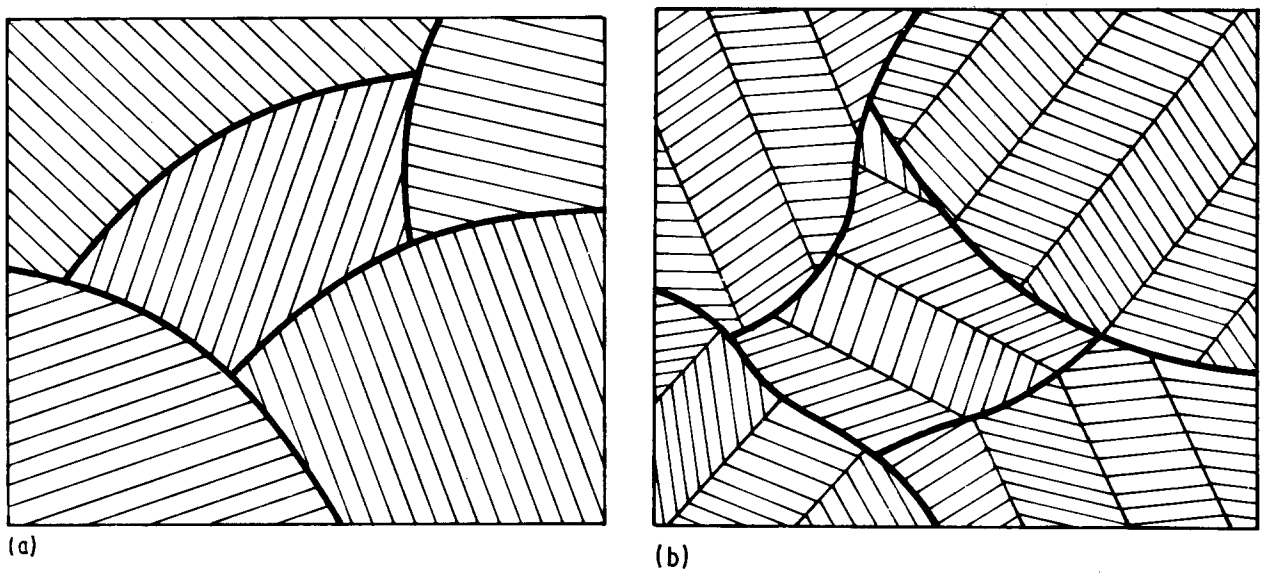

Figure 1 (a) Simple lamellar twinning and (b) banded twin structure in polycrystalline materials.

w_S = surface energy, all energies being expressed as energy density.

In most ferroelectric ceramics, e.g. ($BaTiO_3$) (BT) or ($PbZr_xTi_{1-x}O_3$) (PZT) the domain twinning is such that the electric field energy is negligible, whereas the elastic energy prevails. Therefore the principle of energy minimization is the same as in ferroelastic ceramics and $w_E \approx 0$. The surface energy is certainly negligible as long as the grains are not very fine, or the investigated samples are very thin as in transmission electron microscopy.

Only one calculation of the reduction of elastic energy is known to the author, that published by Willaime and Gandais [9, 10]. They explain twinning for the highly complex example of exsolved alkali feldspar, in which there are alternating lamellae of more potassium-rich monoclinic feldspar and more sodium-rich triclinic feldspar. The slow cooling time of many thousand years of these minerals in nature [12] allows them by twinning to approach a certain degree of a thermodynamic equilibrium with respect to minimizing the internal energy. Here, certainly, chemical energy is involved too. A similar kind of calculation has been proposed by the author for a much simpler case: the domain-splitting in tetragonally distorted perovskite-type ceramics [13, 14] in which elastic matching determines the equilibrium.

2. Mechanical boundary conditions

A slight deformation of the lattice cell by a structural phase transition leads to a slight deformation of the crystallite which is built up of the deformed lattice cells. This deformation, however, is more or less obstructed by the surroundings of the crystallite. A single crystal is free and can therefore in principle deform like the lattice cell. It need not have twins from the mechanical point of view.

A crystallite (grain) in a ceramic is clamped by its neighbouring grains in all three dimensions. It can deform to some degree by cooperative motion of the adjacent grains. Maintaining the shape requires either high internal stresses or mechanical twinning which at least preserves the gross shape of the grain. This will be treated in Section 3.

A crystallite (grain) at the surface of a ceramic body experiences no clamping from the surface. It therefore has different clamping conditions from a grain inside the body and will twin differently. A crystallite (grain) in a thin layer which is thinner than the diameter of the grain is clamped in two dimensions only. Such layers are widely used in transmission electron microscopy.

A crystallite of a thin film on a substrate is also clamped in two dimensions. This clamping is more restricted than that of the free film, because isotropic expansion or contraction of the grains is no longer possible in the two clamping directions and the boundary energy between substrate and layer is also involved.

In addition to these boundary conditions, inhomogeneous internal stresses by mutual interactions between adjacent grains or by inhomogeneous compositions, inhomogeneous cooling through the phase transition, composition-dependent phase transition temperatures and other irregularities will cause additional irregular twinning which is not treated in this paper.

The twinning at the phase transition which (e.g. in the ceramic) maintains the gross shape of the grain may in many materials proceed only in a narrow temperature interval near the phase transition, in which the displaced atoms or the twin boundaries are mobile. At lower temperatures the twin configuration which was formed near the phase transition is either frozen in or subject to further matching when twin boundaries can be moved or generated or annihilated. Transmission electron microscopy reflects the true twin configuration of a ceramic only when this configuration is frozen in and cannot adopt the configuration appropriate to two-dimensional clamping.

The importance of these boundary conditions for the twin configuration is demonstrated in Fig. 2. Fig. 2a shows the domain pattern of well-aged BT. After ageing the ceramic bar was cut by a wire saw and the face of the cut was lapped, polished and etched. The pattern represents the frozen in domain configuration

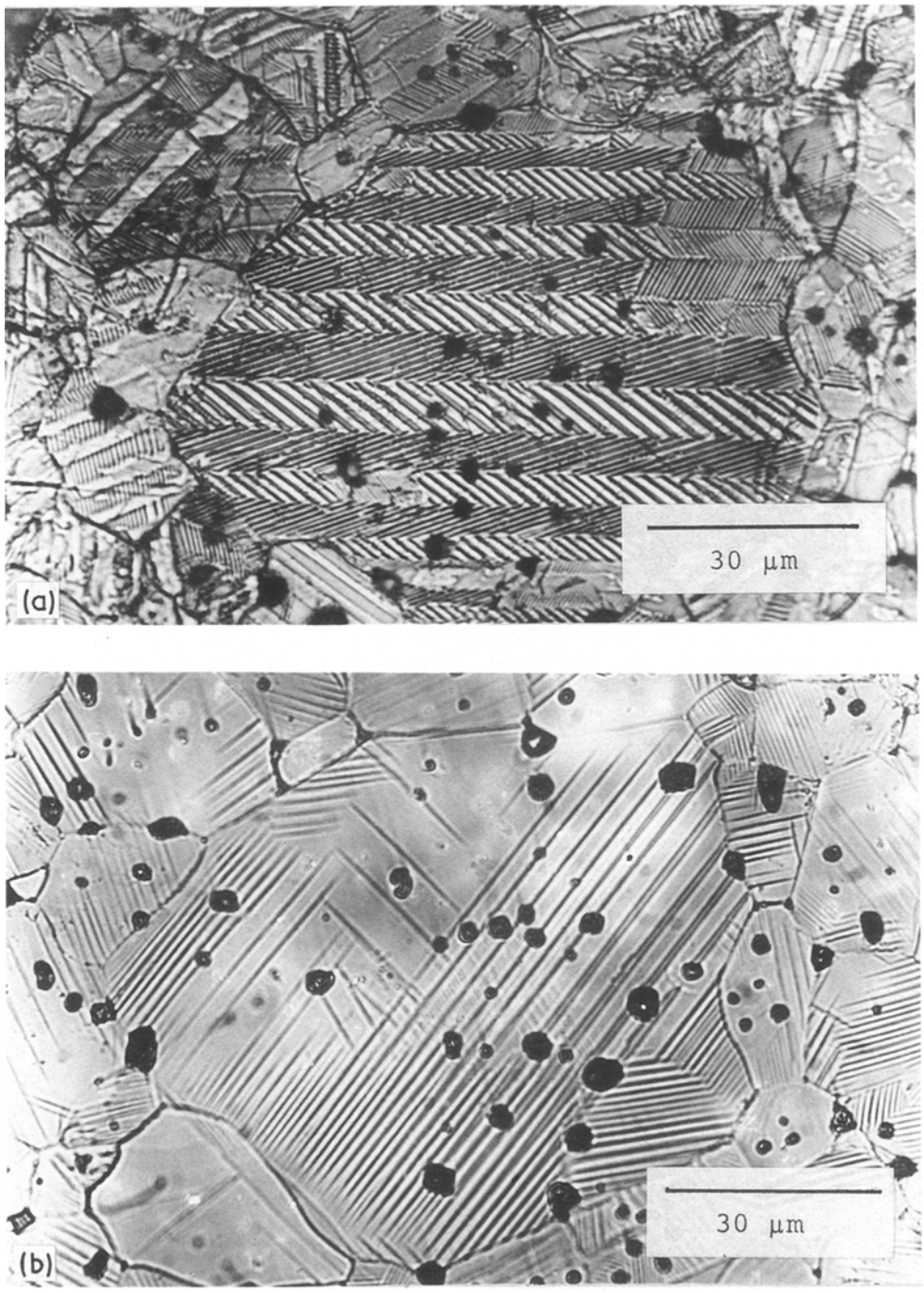

Figure 2 Representative BT domain patterns of a grain: (a) when the pattern is formed inside the ceramic body with three-dimensional clamping, (b) the same grain when the pattern is formed under free surface conditions.

of a grain inside the ceramic, assuming that the mechanical procedure of cutting, lapping and polishing did not modify the frozen-in state. The ceramic was then heated for some time above the transition temperature, cooled to room temperature again, polished and etched. Fig. 2b is the same area as Fig. 2a (slightly shifted and rotated) after this intermediate step of detwinning. The grains at the surface have twinned now under the clamping condition of a grain at the surface. The pattern of Fig. 2b remained unchanged when polished, etched and photographed again three weeks later; thus ageing in this case did not change the domain pattern.

3. Two-dimensional adjustment

The conservation of the shape of the crystallites in the ceramic by twinning is discussed for the example of the ferroelectric phase transition of BT from the cubic phase above about 125° C to the tetragonal phase (c–t) below that temperature. Atoms in the lattice cell are slightly shifted in this transition, which results in a spontaneous polarization P_0 along c and a tetragonal deformation, called spontaneous deformation S_0, which is a strain tensor. In the above example the tensor is

$$S_0 = \begin{pmatrix} S_a & 0 & 0 \\ 0 & S_a & 0 \\ 0 & 0 & S_c \end{pmatrix}$$

where S_a and S_c are the relative changes of the fictitious cubic lattice constant $a_0 = (a^2 c)^{1/3}$;

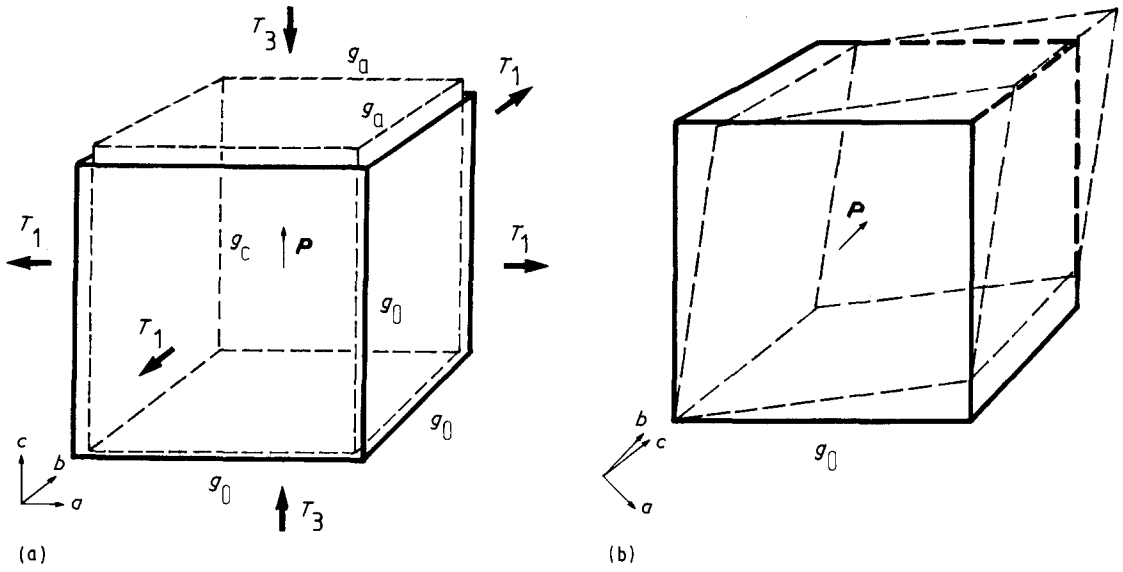

Figure 3 Spontaneous deformation of a cubic grain: (a) the cube edges correspond to the crystallographic axis, (b) the cube edges correspond to a coordinate system rotated 45° around the b axis. In (a) the stress which redeforms the grain to become cubic is indicated.

$S_a = (a - a_0)/a_0$; $S_c = (c - a_0)/a_0$. A cubic grain with grain size g_0 will deform, for example as shown in Fig. 3a or Fig. 3b with dashed lines. The two cases differ only in the crystallographic orientation of the originally cubic grain. By compressional stress T_3 and tensile stress T_1 (as indicated in Fig. 3a) the deformed grain can become a cube again. High stress energies are necessary for this deformation. In the example of $BaTiO_3$ an elementary calculation leads to

$$T_i = \sum c_{ij} S_j \qquad S_1 = S_2 = -S_a + S_x$$
$$S_3 = -S_c + S_x \qquad (1)$$

which yields $T_1 = 190 f_{11}$ MPa and $T_3 = -380 f_{31}$ MPa and the elastic energy density

$$w_1 = 2.08 \times 10^6 N_1 \,\mathrm{J\,m^{-3}} \qquad (2a)$$

In this calculation the grain is deformed by longitudinal stresses only (Fig. 3a). If the spontaneously deformed grain were in a non-distorted isotropic environment, according to Eshelby [15] it would homogeneously deform with about $S_1 = S_2 = -S_a/2$; $S_3 = -S_c/2$ with some inhomogeneous deformation in the environment. This effect is the mechanical analogy of the electric or magnetic "depolarization". The factors f_{11} and f_{31} allow for these reductions. The adjacent grains, however, deform spontaneously too. According to their orientation and deformation they statistically enhance or reduce the necessary strain, which may lead to a further variation of the factors f. In the energy term the factor is called N_1 in order to denote the fact that it includes a "mechanical depolarization" beside the cooperative spontaneous deformation.

Of course under such high deformation it is highly questionable whether the grain still has the same ferroelectric properties as in the free state. P_0 and S_0 were certainly reduced by this deformation, and changes of the crystal structure cannot be excluded. This indeed has been observed as shown below in Fig. 6.

The calculation which leads to Equation 2a is based on the following values for BT at 25° C:

$$c = 4.0361 \times 10^{-10}\,\mathrm{m}$$
$$a = 3.9920 \times 10^{-10}\,\mathrm{m} \qquad a_0 = (a^2 c)^{1/3}$$
$$c_{11}^E = 275x \qquad c_{33}^E = 165x \qquad c_{12}^E = 179x$$
$$c_{13}^E = 151x \qquad c_{44}^E = 54x$$

with $x = 10^9\,\mathrm{N\,m^{-2}}$. A grain like that in Fig. 3b can partly be redeformed by a shear. An energy density

$$w_{Sh} = 1.56 \times 10^6 N_{Sh}\,\mathrm{J\,m^{-3}} \qquad (2b)$$

is necessary for this deformation. The grain then is not yet a cube, because the edge along the b axis is shorter than the two edges of the square at the front of the crystallite. An additional longitudinal deformation is required to make the grain cubic again. The energy for this deformation is calculated below (Equation 2c) to be $w_2 = 0.52 N_2\,\mathrm{J\,m^{-3}}$.

The energy of the electric dipole field of the grain is assumed to be negligible due to the compensation of the polarization charge at the grain boundaries by free charge carriers, e.g. by inversion layers if the voltage between the boundaries is larger than the band gap. The grain as shown in Fig. 3b reduces the high elastic energy by twinning as shown in Fig. 4. In two dimensions its gross shape is now a square $g_1 \times g_1$, the third side remaining g_a. Now a compressive stress $T_1 = T_3 = -95 f_{21}$ MPa and a tensile stress $T_2 = 190 f_{22}$ MPa are required to deform the grain to become cubic with the exception of the serration on two sides. The elastic energy for this deformation is about

$$w_2 = 0.52 \times 10^6 N_2\,\mathrm{J\,m^{-3}} \qquad (2c)$$

The calculation is based on longitudinal deformation only as in the example given above (Equation 1). The elastic constants of the rotated system were used. As long as the twin walls are mobile the grain can accept any shape between the rhombus of Fig. 3b and the rhombus with the other face diagonal.

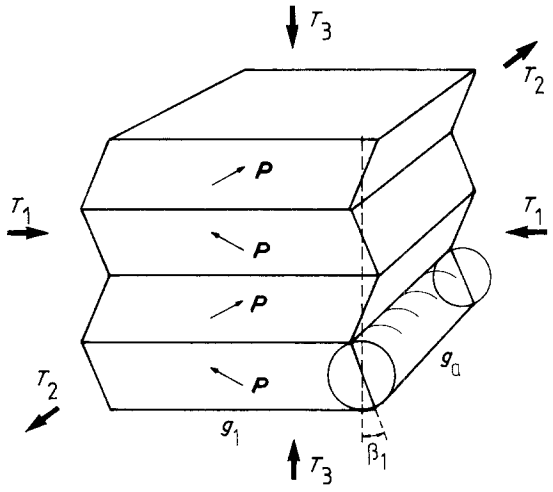

Figure 4 The spontaneous deformation as shown in Fig. 3b is reduced by twinning. Serration appears at the grain boundary. Homogeneous stresses T as indicated can restore the gross cubic shape.

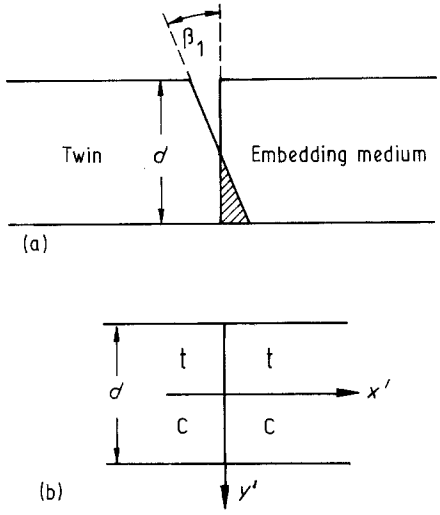

Figure 5 Deformation at a grain boundary: (a) a twin and its adjacent embedding medium if cleft, (b) compressional (c) and tensile (t) stress regions in the uncleft boundary.

If the wall motion is reversible then it will contribute to the elastic and/or dielectric behaviour of the ceramic [14, 16, 17]. In twinned metals this elastic effect was observed first by Worrel [18] and Zener [19] and later by many other authors (e.g. [20]). Superelasticity is based on such reversible motions [7, 20].

In BT the twin boundaries are $\{1\,1\,0\}$ planes of the pseudo-cubic lattice. By this kind of twinning no polarization charge appears at the interfaces and therefore the electric field energy is zero. Nevertheless the twin boundary or domain wall has a surface energy per unit area σ_{90}.

The twin width d in the arrangement of Fig. 4 is governed by the minimum of the total energy density, which is the sum of elastic energy and domain wall energy. The elastic energy is the sum of w_2 and the strain energy caused by the serration at the grain boundaries.

To estimate this energy we suppose the grain to be embedded in an isotropic elastic matrix, which has the same representative elastic constant c as the grain. If the boundary between the twin lamellae and the embedding medium were cleft we would find an overlapping region in the lower part and a wedge-shaped slit in the upper part between the two as shown in Fig. 5a. In the unsplit boundary (Fig. 5b) we find compressional stress c in the lower half and tensile stress t in the upper half of the boundary. Instead of solving the differential equation for this complicated elastic problem, the elastic energy in this region is estimated by a simple model.

The longitudinal strain in this model has only the S_{xx} component which decreases exponentially toward both sides of the boundary, with a penetration depth $d/2$:

$$S_{xx} = S_1 \, e^{-2|x'|/d} \tag{3a}$$

S_1 is chosen such that the total displacement along a path from $x = -\infty$ to $x = +\infty$ at constant y' corresponds to the width of the slit with respect to the overlapping at this y' site:

$$S_1 = \frac{\beta_1 y'}{d} \tag{3b}$$

The local energy density along a path parallel to the x'-axis then is

$$w_s = \tfrac{1}{2} c \frac{\beta_1^2 y'^2}{d^2} e^{-4|x'|/d}$$

with the representative elastic constant c. To get the total energy per unit length h (which is perpendicular to the plane of drawing) we have to integrate along x' from $-\infty$ to $+\infty$ and along y from $-d/2$ to $+d/2$:

$$\frac{W_s}{h} = \frac{1}{2} \frac{c\beta_1^2}{d^2} \int_{-d/2}^{+d/2} \int_{-\infty}^{+\infty} y'^2 \, e^{-4|x'|/d} \, dx' \, dy'$$

$$= \tfrac{1}{48} c\beta_1^2 d^2 \tag{4}$$

The elastic energy in this part of the boundary, which is indicated by the cylinder in Fig. 4, is

$$W_s = kc\beta_1^2 d^2 g \tag{5}$$

Any other simplified or correct mathematical treatment of the elastic energy for smoothing the rippled deformation leads to Equation 5 with other factors k and c which depend on the model. The above crude model gives with $kc = c_{11}/48$ an order-of-magnitude estimate. By comparison with measured results a matching of kc leads to values around $0.5 \times 10^9 \, N\,m^{-2} \approx kc$ which is about 6 times smaller than $c_{11}/48$ as estimated by the model ($c_{11} \approx 1.5 \times 10^{11} \, N\,m^{-2}$ as for ceramics).

Since we have g/d deformations on both sides of the cube the total energy stored there is $W_{SR_1} = 2W_s g/d$. The energy density w_{SR_1} of the grain becomes

$$w_{SR_1} = 2kc\beta_1^2 d/g \tag{6}$$

This inhomogeneous elastic energy is concentrated in the boundary region within a layer of thickness d, and with maximal strain values $\pm\beta_1/2$ at $x' = 0$, $y' = \pm d/2$.

The total energy density caused by the surface energy of the domain walls is

$$w_{w_{90}} = \sigma_{90}/d \tag{7}$$

if σ_{90} is the domain wall energy per unit area. The minimum condition for the sum of Equations 2, 6 and

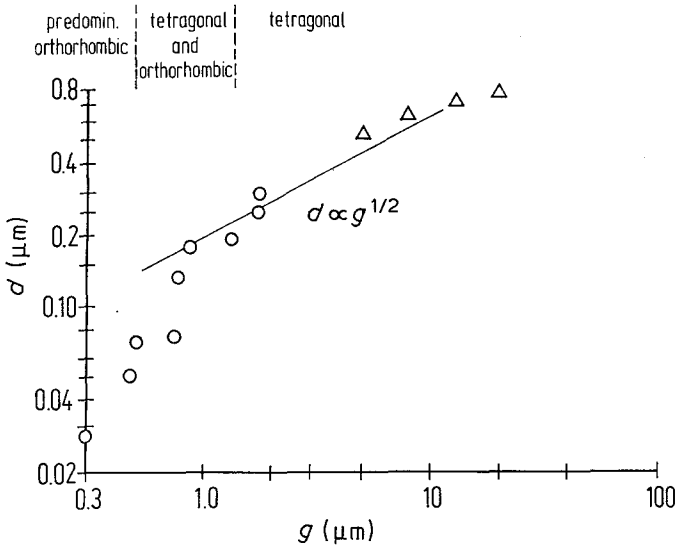

Figure 6 Domain width of BT as a function of grain size measured with (△) light microscopy and (○) electron microscopy. The spontaneous strain is strongly reduced at small grain size and the crystallographic structure is no longer unique in this region with $g < 1\,\mu m$.

7 leads to the equilibrium domain width d (w_2 is independent of d) given by

$$d = \left(\frac{\sigma_{90} g}{2kc\beta_1^2}\right)^{1/2} \tag{8}$$

and to the minimum energy

$$w_{\min_1} = w_2 + \left(\frac{8k\sigma_{90} c\beta_1^2}{g}\right)^{1/2} \tag{9}$$

Here the first term represents the homogeneous stress energy in the grain (Equation 2c); the second term is half domain-wall and half elastic energy in the serrated boundary.

An interesting result is the dependence of the twin width d on the grain size $d \propto g^{1/2}$. This relationship is not restricted to $BaTiO_3$. It holds for all kinds of simple lamellar twinning in metals and ceramics in which the twin wall energy σ and the elastic deformation energy w_{SR_1} determine the minimum. It does not depend on the kind of interface which separates the twins. Nature certainly will favour twin boundaries with low energies. Plastic deformation as known from metals will possibly modify the results. Fig. 4 shows clearly that the shape adjustment by simple lamellar twinning is in two dimensions only. The relationship of Equation 8 has indeed been confirmed in fine-grained BT ceramics [14] for grain sizes between 1 and 10 μm as shown in Fig. 6.

If the grain size is smaller than about 1 μm a change of the crystallographic structure of BT and a reduction of the spontaneous deformation are observed. Then both σ_{90} and β_1 are dependent on the structure and will lead to a modified equilibrium. In addition the electric energy and the surface energy of the very fine grains can presumably no longer be neglected.

It is interesting to extrapolate Equation 8 to that grain size g_{crit_1} which is identical with the domain width d, discarding the physical effects cited above for fine grains:

$$g_{crit_1} = \frac{\sigma_{90}}{2kc\beta_1^2} \tag{10}$$

Below this fictitious grain size no domain twinning would occur. The grain does not yet contain enough elastic energy for an energy-reducing splitting by a wall with energy σ_{90}. This critical grain size finds a very simple explanation as demonstrated in Fig. 7. With homogeneous stress in the grain, the absolute stress energy increases with grain size $\propto g^3$. Any kind of domain wall energy increases $\propto g^2$. Only at or above the point of intersection of the two curves (Fig. 7a) is there enough energy to create a twin. The second term in Equation 9 which describes the twinning energy then becomes

$$w_{crit_1} = 4kc\beta_1^2 \tag{11}$$

This energy should be comparable with the deformation energy as given by Equation 2b. If the deformation factor is tentatively $N_{Sh} \approx 0.13$ then from this comparison

$$N_{Sh}\, w_{Sh} = w_{crit_1}$$

kc can be estimated for BT to be

$$kc \approx 0.5 \times 10^9\ \mathrm{N\,m^{-2}} \tag{12}$$

with $\beta_1 \approx (c/a) - 1 \approx S_c - S_a = 1.1 \times 10^{-2}$.

A comparision of Equation 8 with the measured values of grain size and domain width [14] (see Fig. 6), e.g. $g = 10\,\mu m$ and $d = 0.65\,\mu m$, leads to a domain wall energy $\sigma_{90} = 5.1 \times 10^{-3}\,\mathrm{J\,m^{-2}}$ assuming kc as given by Equation 12. This value for σ_{90} is near that calculated by Zhirnov [21] ($\sigma_{90} = 2$ to $4 \times 10^{-3}\,\mathrm{J\,m^{-2}}$) and by Bulaewski [22] ($\sigma_{90} = 3.4 \times 10^{-3}\,\mathrm{J\,m^{-2}}$); it is lower than that given by Kittel [23] ($\sigma_{90} \approx 10^{-1}\,\mathrm{J\,m^{-2}}$). This agreement and the observed $d \propto g^{1/2}$ dependence are a confirmation of the model. The fictitious critical grain size according to Equation 10 is then $g_{crit_1} \approx 40\,nm$.

The two-dimensional grain adjustment as described above can occur in cubic–tetragonal transitions of fine-grained ceramics (coarse grains are discussed in the next Section), in thin films where clamping in the third direction is not required, or in the tetragonal–orthorhombic transition of the high-T_c superconducting ceramics. Figs 8 and 9 show SEM photographs and light micrographs of fine- and coarse-grained BT and the high-T_c superconductor $YBa_2Cu_3O_{7-\delta}$. In BT the domain configuration which is established at the transition

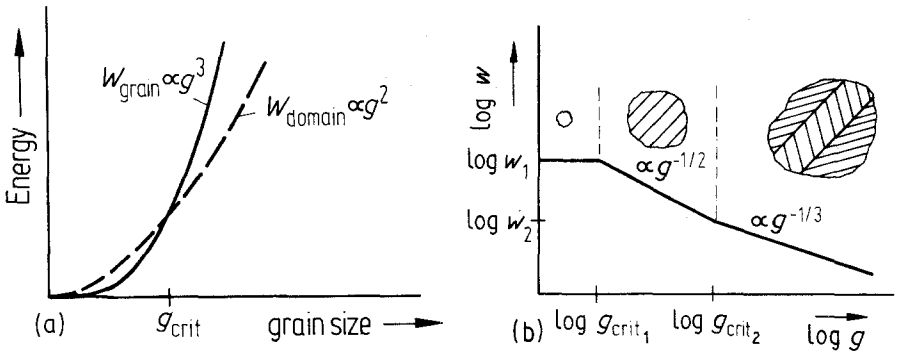

Figure 7 (a) The homogeneous elastic energy in the grain increases with g^3, the domain wall or interface energy increases with g^2. The intersection of both curves determines the lower limit for g_{crit}. (b) Dependence of the elastic energy density w on grain size g (schematically).

temperature of about 125° C is very mobile some 10 K below T_c [24]. Below 100° C, however, it becomes almost frozen in and can vary only slowly or only if stresses larger than a coercive stress modify the configuration towards lower energy.

In $YBa_2Cu_3O_{7-\delta}$, the phase transformation at about 700 to 600° C, which is t–o, leads with oxygen diffusion [8, 9] to an adjustment by twinning of the plate-like grains in the plane perpendicular to c. The diameter of the plate-like grains corresponds to our grain size g in the preceding discussion. The mobility at these temperatures is sufficient to establish the domain configuration.

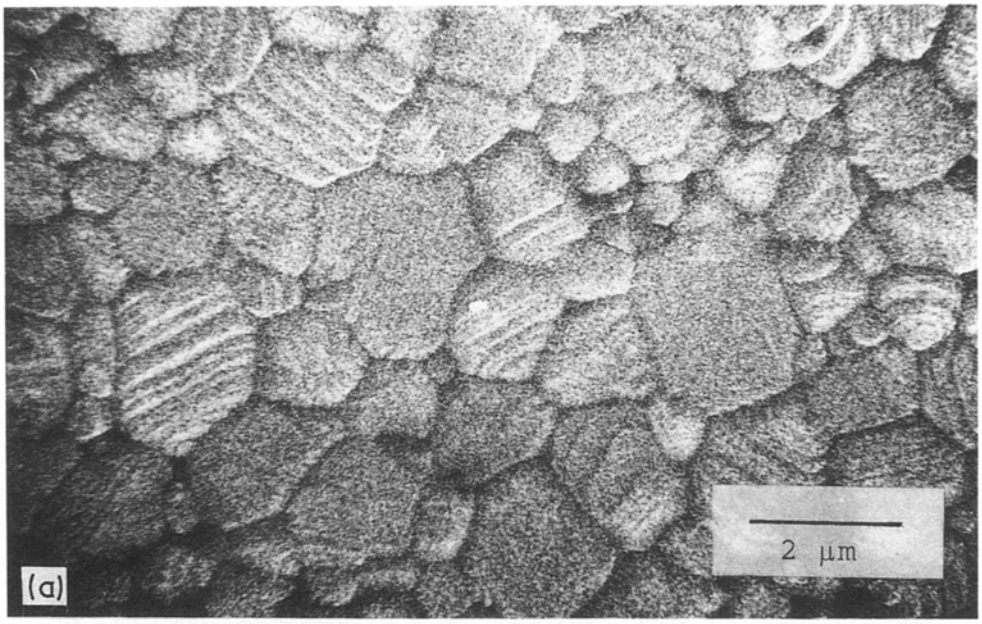

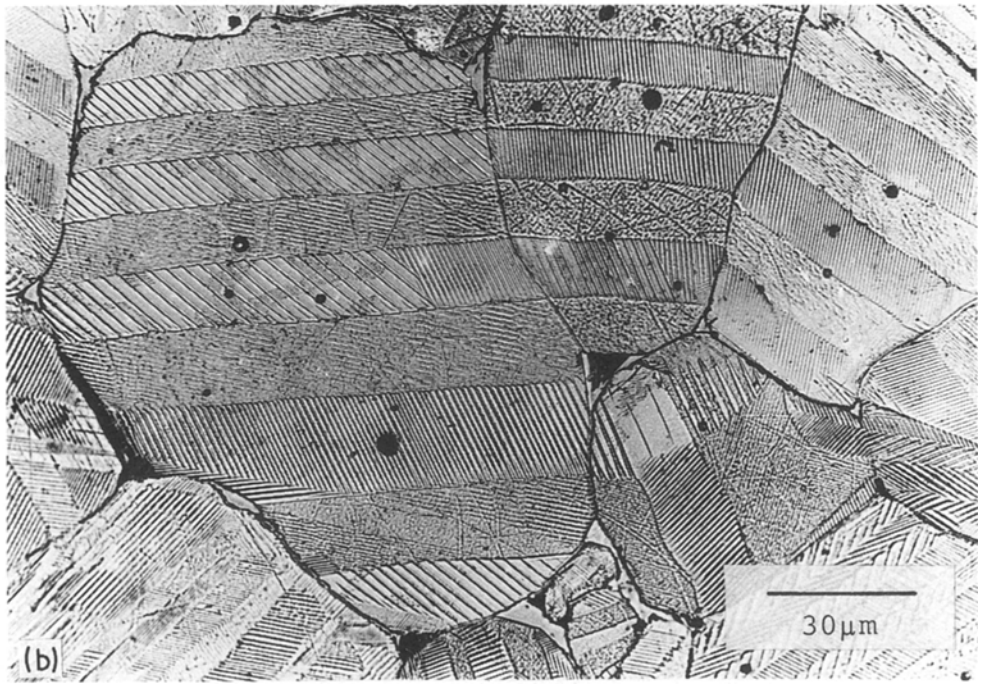

Figure 8 (a) Scanning electron micrograph of fine-grained BT. (b) Light micrograph of coarse-grained BT.

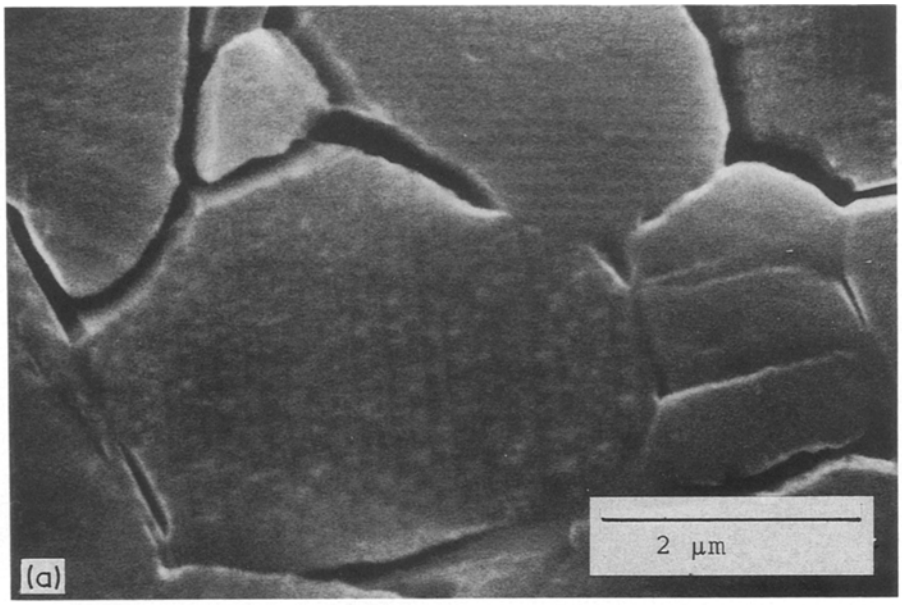

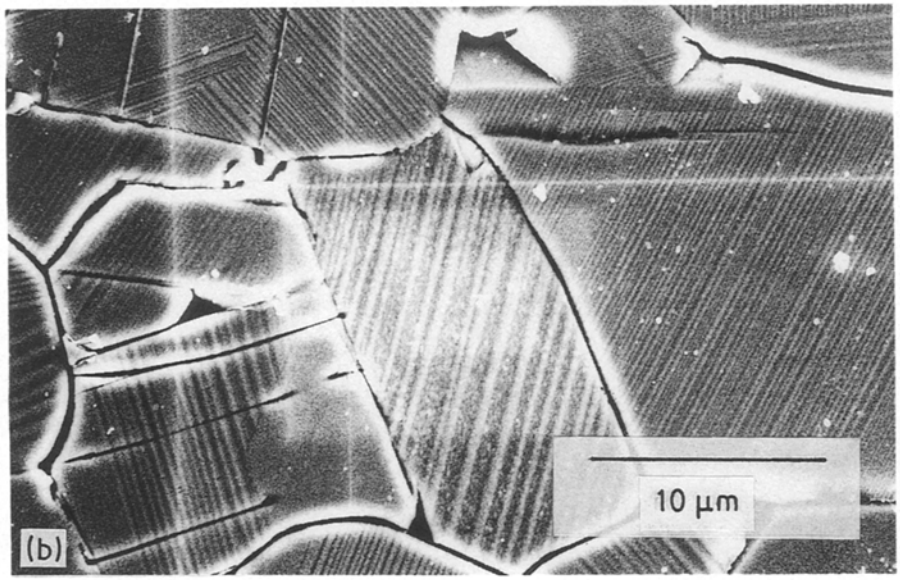

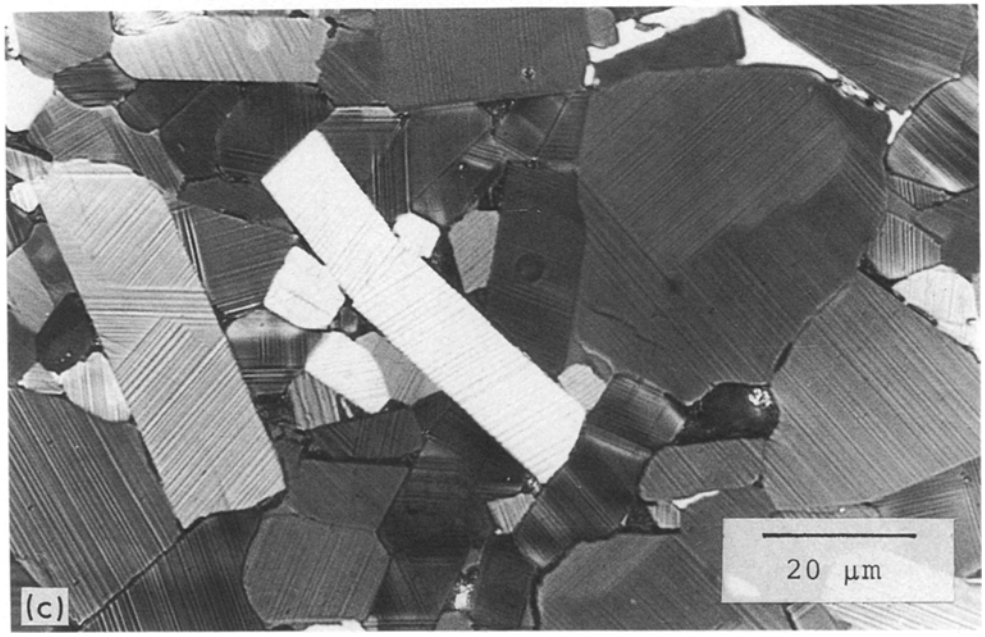

Figure 9 (a) Scanning electron micrograph of fine-grained YBaCuO. (b) Scanning electron micrograph of medium-grained YBaCuO. (c) Polarized light micrograph of coarse-grained YBaCuO.

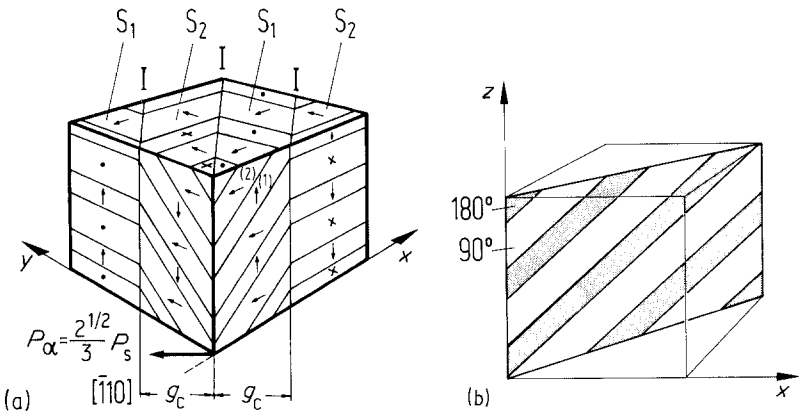

Figure 10 (a) Domain configuration (α-type) in coarse-grained BT ceramics. Banded stacks S_1, S_2 with critical width g_c separated by interfaces I appear at the surface. Inside the cube there is no polarization charge. (b) The interfaces I are alternating stripes of 90° and 180° domain walls.

Thus with slow cooling a certain orthorhombic state from 500° C or higher is frozen in. Further chemical reaction with oxygen combined with some variation of the b/a value [8, 9] will not change the gross domain configuration. Instead there may be a generation of finer domains down to a width of 30 nm [25, 26] depending on local stress situations. This irregular domain-twinning does not fit the above discussion. It is not clear whether the very fine domains seen with TEM in thin layers exist in three-dimensionally clamped ceramic grains.

4. Three-dimensional adjustment

The c–t transition, as for instance in BT, allows all {1 1 0} planes to become domain walls. Therefore a further stress relief by another kind of interface which brings relief in the third dimension is possible.

In contrast $YBa_2Cu_3O_{7-\delta}$ allows twinning at (1 1 0) and (1 $\bar{1}$ 0) pseudo-tetragonal planes only with low energy. There seems to be almost no twinning which effects grain adjustment in the c direction. Shrinking in the c direction is therefore not compensated by twinning. Microcracks parallel to (0 0 1) as revealed in Fig. 9b are a consequence.

Coarse-grained BT ceramic has the banded structure shown in Figs 8b and 2a. Its domain configuration has been determined [13]. Fig. 10 schematically shows the α-type of this twinning. New interfaces I consisting of alternating 90° walls and 180° walls between stacks S_1 and S_2 of simple twin lamellae allow a grain adjustment in the third dimension, and inhibit polarization fields. The β-type twinning with polarization fields [13] will not be discussed here. The grain is now a cube if those twins which meet at the interface I with 180° walls have a width of $d/2$ compared with the twins of width d which meet at the 90° walls of the interface.

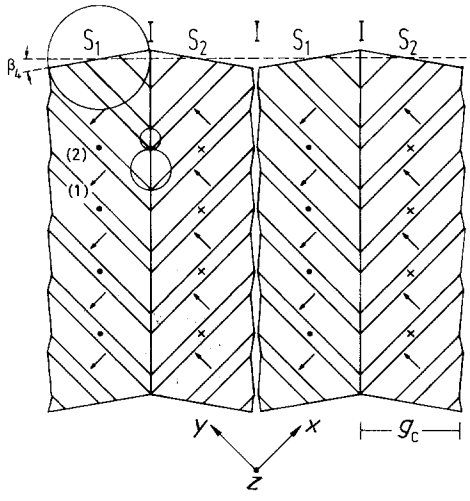

Figure 11 The surface of the grain of Fig. 10a seen from the z direction, with idealized cleavage in one of the interfaces. The small circles represent a characteristic region of elastic energy as explained in Fig. 12. The large circle indicates a similar type of elastic energy as shown in Fig. 4 which can be treated with Equation 5 if d and β_1 are replaced by g_c and β_4.

The interface I in addition to its normal domain wall energy σ_{90} and σ_{180} is a carrier of elastic energy which results from the deformation as discussed in Section 3. Fig. 11 represents the grain of Fig. 10a seen from the z direction, if it were split at one of the interfaces. The deformation at the two smaller circles of Fig. 11 is repeated in Fig. 12. A geometrical analysis leads to $\beta_2 = \frac{1}{3}\beta_1$; $\beta_3 = \frac{2}{3}\beta_1$ and for the deformation at the boundary (large circle in Fig. 10) one gets $\beta_4 = \frac{1}{3}\beta_1$.

By using these angles the elastic energy of the interface can now be estimated with the same method as used in Section 3. With Equation 4 the elastic interface energy per unit area is

$$\sigma_1 = \frac{8(2)^{1/2}}{27} k_1 c_1 \beta_1^2 d \qquad (13)$$

Compared with this energy the domain wall contributions σ_{90} and σ_{180} are small enough to be neglected. k_1 and c_1 certainly differ from k and c since the geometrical structure of the deformation in the interface

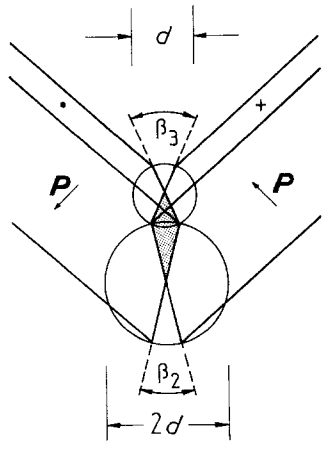

Figure 12 The small circled regions of Fig. 11, shown in the idealized cleft state.

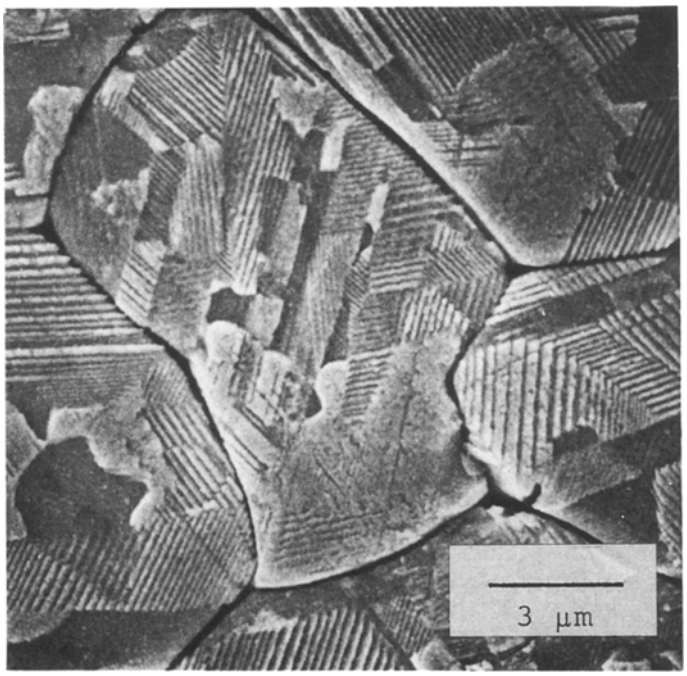

Figure 13 Scanning electron micrograph of PZT.

and the elastic constants are somewhat different to that of the simple model which leads to Equation 5.

The serrated grain boundary (large circle in Fig. 11) with serration period g_c is smoothed by elastic deformation of the grain and the embedding medium. The elastic energy for smoothing is stored in a layer of thickness g_c on both sides of the grain boundary. The energy density of the grain of volume g^3 is then

$$w_{SR_2} = \frac{2kc\beta_1^2 g_c}{9g} \quad (14)$$

Grains which are larger than g_c allow in addition a cooperation of grains by serrated edges at the grain boundary. This can be seen in Fig. 8b as bands which extend over many grains. The effect will decrease the energy given by Equation 14. Since it cannot easily be quantified the further calculation is based on Equation 14.

The calculation of the minimum of the sum of both energy densities (Equation 13) with $w_{w_1} = \sigma_1/g_c$ and Equation 14,

$$w_{w_1} + w_{SR_2} = \text{minimum} = w_{min_2} \quad (15)$$

leads to the interface distance g_c. Furthermore the total energy which is the minimum of Equation 15 and the domain wall energy (Equation 7),

$$w_{min_2} + \frac{4}{3}\frac{\sigma_{90}}{d} = \text{minimum} \quad (16)$$

has to be minimized with respect to d. This results in the equilibrium values $d(g)$ and $g_c(g)$ and the total energy density $w_{tot_{min}}$:

$$d = \left(\frac{27\sigma_{90}^2 g}{2^{1/2}\beta_1^4 k_1 c_1 kc}\right)^{1/3} \qquad d \propto g^{1/3} \quad (17)$$

$$g_c = \left(\frac{8(2)^{1/2} k_1 c_1 \sigma_{90} g^2}{(kc)^2 \beta_1^2}\right)^{1/3} \qquad g_c \propto g^{2/3} \quad (18)$$

$$w_{tot_{min}} = \frac{4}{3}\left(\frac{2^{1/2} k_1 c_1 kc\ \beta_1^4 \sigma_{90}}{g}\right)^{1/3} \qquad w_{tot_{min}} \propto g^{-1/3} \quad (19)$$

$d(g)$ as given by Equation 17 is roughly in agreement with the experimental results in the banded structure [14]. Equation 18 gives the order of magnitude of the width of the bands of known domain patterns. Although g_c values have never been systematically investigated, experience tells us that the width of the bands g_c in BT varies between 5 and 20 μm in unpolarized BT ceramics. According to experience g_c seems to be not so strongly dependent on grain size as given by Equation 18. The number of bands per grain is not very large; in addition, statistical scatter resulting from individual sites and shapes and orientations of the grains and of the embedding situation and from different cooling procedures may be the origin of deviations from Equation 18.

The critical grain size g_{crit_2} above which three-dimensional adjustment occurs (Fig. 7) is derived from Equation 18 with $g_c = g = g_{crit_2}$:

$$g_{crit_2} = \frac{8(2)^{1/2} k_1 c_1 \sigma_{90}}{(kc)^2 \beta_1^2} \quad (20)$$

With $kc = 0.5 \times 10^9\,\mathrm{J\,m^{-3}}$ as before and $k_1 c_1 = 2.5 \times 10^9\,\mathrm{J\,m^{-3}}$, $\sigma_{90} = 5.1 \times 10^{-3}\,\mathrm{J\,m^{-2}}$ and $\beta_1 = 1.1 \times 10^{-2}$ this critical grain size is about 4.7 μm. The domain width for $g = 100\,\mu$m from Equation 17 is $d = 1.4\,\mu$m. The width of the bands for $g = 100\,\mu$m from Equation 18 is $g_c = 36\,\mu$m, which certainly is too large. The discrepancy is certainly not only caused by the incorrectness of almost all parameters in Equation 20. The model has to be refined in order to give better agreement in some details.

The total energy at the critical grain size g_{crit_2} is

$$w_{crit_2} = \tfrac{2}{3}\, kc\beta_1^2 \quad (21)$$

This energy density again can be compared with Equation 2c and leads to the factor $N_2 \approx 0.07$ for the cooperation of adjacent grains and for mechanical depolarization. The accuracy of this figure is certainly low.

Similar banded structures (Fig. 13) are seen in lead–zirconate–titanate (PZT) which has a c–t structural

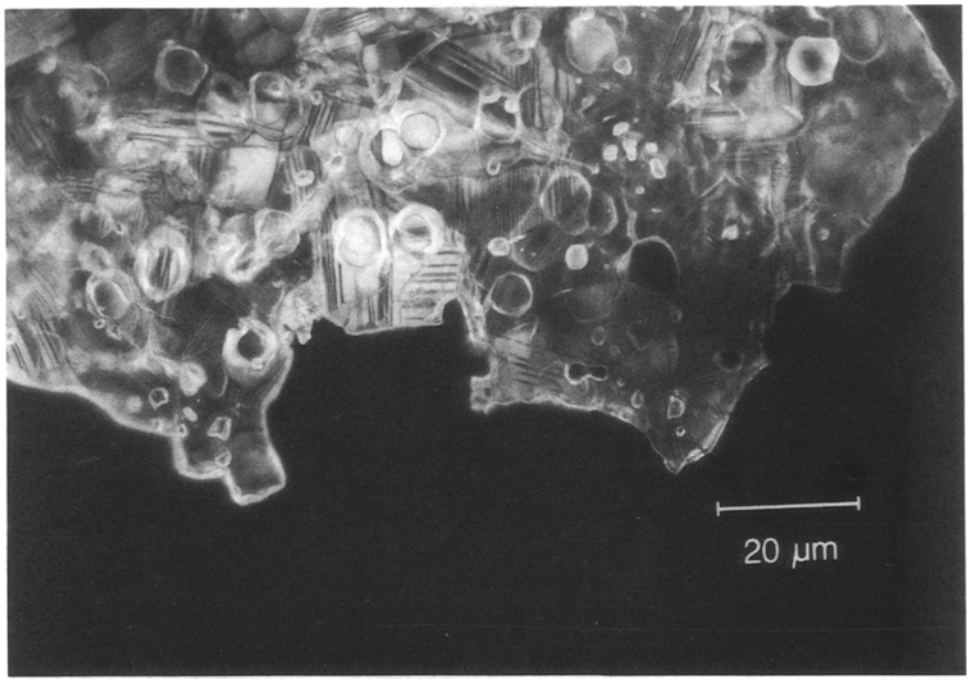

Figure 14 Thinned region of a coarse-grained BT ceramic (polarized light micrograph).

phase transition like BT at about 400° C. The observed domain width d and the width of the bands g_c are about 3 to 10 times smaller than those of BT. The three-times larger spontaneous polarization in PZT and the smaller grain size ($\sim 10\,\mu m$) point with Equations 17 and 18 to this reduction of d and g_c. Nothing, however, is known about the energy σ_{90} of the domain walls in PZT.

The domain patterns of orthorhombic or rhombohedral BT or other perovskites are not well known. Various simple lamellar regions exist in each grain. It is unknown whether a regular kind of interface – planar or non-planar – exists for three-dimensional adjustment.

Fig. 14 shows a light micrograph of a coarse-grained sample of BT which was thinned by ion bombardment for transmission electron microscopy. As mentioned before, thin layers require a two-dimensional adjustment only. The sample shown in Fig. 14 indeed shows only simple lamellar twinning although it is coarse-grained. The surface is damaged by the ion etching.

5. Irregular domain structures

Most single crystals contain some 90° domain twinning (in addition to 180° twinning which is not of interest here) unless the domain walls are removed by electric and/or elastic fields. This at a first sight contradicts the expectations. If we realize, however, that even a perfect crystal does not cool homogeneously through the transition temperature and therefore develops internal stresses, we can understand the domain formation as a process for the reduction of elastic energy. In addition, different types of crystallographic defect create stress fields which can be reduced by twinning.

With transmission electron microscopy [25–29] much finer twins, which do not fit the considerations of the preceding sections are observed in ceramics and in single crystals. The micrographs which are published show clearly that these fine domains are not a regular substructure of the domain pattern described above. One can assume that these twins are caused by local and inhomogeneous stresses which can have different origins. Some of these have already been mentioned: inhomogeneous stresses by adjacent grains, inhomogeneous cooling, inhomogeneous composition, dislocations. It is certainly a challenge to understand these irregular configurations.

The spontaneous strain furthermore increases with decreasing temperature. Thus a domain configuration which is frozen in at a higher temperature and which gives stress relief at this temperature is under new stress at lower temperatures. There is not enough knowledge about domain wall mobility and domain nucleation to understand how further stress relief at temperatures much below the transition proceeds, and whether the fine domains are a product of this process.

6. Conclusion

Twinning in $BaTiO_3$ ceramics effects relief of stress which has its origin in a structural phase transition. It proceeds in two steps: in fine-grained ceramic the deformed grains adjust in two dimensions by simple lamellar twinning, in coarse-grained ceramic a second kind of twinning with more complicated interfaces allows grain adjustment in the third dimension as well.

The calculation of the average twin size and the width of the bands is based on a simplified stress distribution near the serrated edges. It leads to results which agree roughly with experience. Since the model applied here is more general it will be applicable also to other materials than ferroelectric ceramics: generally to those in which the elastic energy has to be reduced and which can form interfaces with energies low enough to reduce the overall elastic energy. The model is restricted to polycrystalline materials in which the grains are clamped or partly clamped by

adjacent grains. In thin films only the first step of twinning is necessary since the grains are clamped in the plane of the film only.

Acknowledgements

I thank the Philips Research Laboratories Aachen, the Gemeinschaftslabor für Elektronenmikroskopie of Aachen University of Technology, Professor Dr Ho-Gi Kim of Korea Advanced Institute of Science and Technology and Mrs D. Leisten of our laboratory for the various micrographs.

References

1. R. W. CAHN, *Adv. Phys.* **3** (1954) 363.
2. J. W. CHRISTIAN, in "The Mechanism of Phase Transformations in Crystalline Solids", Monograph and Report Series Vol. 33 (Institute of Metals, London, 1969) p. 129.
3. C. M. WAYMANN, in "Diffraction and Imaging Technique in Materials Science", edited by S. Amelinckx, R. Gevers and I. van Landuyt (North Holland, 1978) pp. 251ff.
4. A. JOHNSON, "Neues Jahrbuch Mineralogie", Beilageband 39 (1914) p. 500.
5. K. AIZU, *J. Phys. Soc. Jpn* **27** (1969) 387.
6. *Idem, ibid.* **32** (1971) 1959.
7. L. S. FOMENKO, S. V. LUBENETS and V. I. STARTSEV, *Scripta Metall.* **18** (1984) 535.
8. H. M. O'BRYAN and P. K. GALLAGHER, *Adv. Ceram. Mater.* **2** (1987) 640.
9. T. J. KISTENMACHER, *J. Appl. Phys.* **64** (1988) 5067.
10. C. WILLAIME and M. GANDAIS, *Phys. Status Solidi (a)* **9** (1972) 529.
11. C. WILLAIME, W. L. BROWN and M. GANDAIS, in "Electron Microscopy", edited by H.-R Wenk (Springer, Berlin, 1976) Ch. 4.9.
12. P. E. CHAMPNESS and G. W. LORIMER, *ibid.* Ch. 4.1.
13. G. ARLT and P. SASKO, *J. Appl. Phys.* **51** (1980) 4956.
14. G. ARLT, D. HENNINGS and G. de WITH, *ibid.* **58** (1985) 1619.
15. J. D. ESHELBY, in 'Progress in Solid Mechanics", Vol. 2 (North-Holland, Amsterdam, 1961) pp. 89–140.
16. G. ARLT, H. DEDERICHS and R. HERBIET, *Ferroelectrics* **74** (1987) 37.
17. O. M. ZHANG *et al.*, *J. Appl. Phys.* **64** (1988) 6445.
18. P. T. WORRELL, *ibid.* **19** (1948) 927.
19. C. ZENER, "Elasticity and Anelasticity in Metals", (University Press, Chicago, 1948) p. 159.
20. J. W. CHRISTIAN, *Metall. Trans. A* **13A** (1982) 509.
21. V. A. ZHIRNOV, *Sov. Phys. JETP* **35** (1959) 822.
22. L. N. BULAEWSKI, *Sov. Phys. Sol. State* **5** (1964) 2329.
23. C. KITTEL, *Sol. State Commun.* **10** (1972) 119.
24. M. DISTELHORST, R. HOFMANN and H. BEIGE, *Jap. J. Appl. Phys.* **24** (1985) Suppl. **24-2** (1985) 1019.
25. J. F. SMITH and D. WOHLLEBEN, *Z. Phys. B Cond. Matt.* **72** (1988) 323.
26. G. v. TENDELOO, H. W. ZANDBERGEN and S. AMELINCKX, *Sol. State Commun.* **63** (1987) 603.
27. M. TANAKA and G. HONJO, *J. Phys. Soc. Jpn* **19** (1964) 954.
28. T. MALIS and H. GLEITER, *J. Appl. Phys.* **47** (1976) 5195.
29. Y. J. CHANG, *Appl. Phys.* **A29** (1982) 237.

Received 3 July
and accepted 16 August 1989